Prog. Theor. Exp. Phys. **2019**, 053E03 (14 pages)
DOI: 10.1093/ptep/ptz039

Probing Planck-scale spacetime by cavity opto-atomic ^{87}Rb interferometry

Mohsen Khodadi,[1,*] Kourosh Nozari,[1,2,*] Anha Bhat,[3,*] and Sina Mohsenian[4]

[1]*Department of Physics, Faculty of Basic Sciences, University of Mazandaran, 47416-95447, Babolsar, Iran*

[2]*Research Institute for Astronomy and Astrophysics of Maragha (RIAAM), 55134-441, Maragha, Iran*

[3]*Department of Metallurgical and Materials Engineering, National Institute of Technology, Srinagar 190006, India*

[4]*Department of Mechanical Engineering, University of Massachusetts Lowell, Lowell, MA 01854, USA*

[*]E-mail: m.khodadi@stu.umz.ac.ir, knozari@umz.ac.ir (Corresponding Author), anhajan1@gmail.com

Received December 29, 2018; Revised February 20, 2019; Accepted March 5, 2019; Published May 30, 2019

The project of *quantum spacetime phenomenology* focuses on searching pragmatically for the Planck-scale quantum features of spacetime. Among these features is the existence of a characteristic length scale commonly addressed by effective approaches to quantum gravity (QG). This characteristic length scale could be simply realized, for instance, by generalizing the standard Heisenberg uncertainty principle to a *generalized uncertainty principle* (GUP). While it is usually expected that phenomena belonging to the realm of QG are essentially probable solely at the so-called Planck energy, here we show how a GUP proposal containing the most general modification of coordinate representation of the momentum operator could be probed by a *cold atomic ensemble recoil experiment* (CARE) as a low-energy quantum system. This proposed atomic interferometer setup has advantages over the conventional architectures owing to the enclosure in a high-finesse optical cavity that is supported by a new class of low-power-consumption integrated devices known as *micro-electro-opto-mechanical systems*. In the framework of a top-down-inspired bottom-up QG phenomenological viewpoint and by taking into account the measurement accuracy realized for the fine structure constant from the rubidium (^{87}Rb) CARE, we set some constraints as upper bounds on the characteristic parameters of the underlying GUP. In the case of superposition of the possible GUP modification terms, we managed to set a tight constraint of $0.999\,978 < \lambda_0 < 1.000\,02$ for the dimensionless characteristic parameter. Our study shows that the best playground to test QG approaches is not merely high-energy physics, but a table-top nanosystem assembly as well.
PACS numbers: 04.60.-m, 04.60.Bc

Subject Index E05

1. Introduction

Despite three well tested and powerful theories—quantum field theory (QFT), the standard model of particles (SM), and general relativity (GR)—our theoretical framework for studying the universe is incomplete for two main reasons. The primary reason is that no well formulated quantum gravity (QG) theory that unifies the micro-level universe (subjected to quantum mechanics (QM)) and Einstein's theory of gravity (relevant to the macro-level universe) has been constructed properly so far. The secondary reason is the lack of a well established framework for the unification of gravity with three other fundamental interactions. The root of this incomplete issue comes back to substantive differences between QM and GR, which are well discussed in, for instance, Refs. [1,2]. Nowadays, there is great curiosity in the theoretical physics community about understanding the physics of the Planck scale, which is considered to be one of the challenging research areas. Given that QM quantizes any dynamical field as well as its physical content, so QG would be related to the discreteness of geometrical concepts such as length, area, and volume. This implies that the combination of the relativistic and quantum effects results in reshaping of the common concept of distance around the natural scale known as the *Planck scale* $\ell_\mathrm{p} \approx 10^{-35}$ m. Although a fully functional unified QG theory has remained out of reach for less than a century, there are, however, some convincing approaches available such as string theory [3,4], canonical quantum gravity [5,6], various models of deformed special relativity (DSR) [7,8], and also a variety of generalized uncertainty principles (GUP) [9,10], which seem to be potential candidates for converging the study. These approaches implicitly predict a fundamentally quantized space due to the existence of a minimal uncertainty in physical distance Δx_{min} of the order of the Planck length ℓ_p. In fact, Einstein's perspective on gravity as a property of spacetime, and not merely as a usual force, has led to the creation of an effective framework for QG with the impression that a quantum particle is moving on a spacetime with a geometry equipped with a fundamental, minimal characteristic length. It can be easily shown that the minimal length uncertainty results in a modification of the standard canonical commutation relations (CCR) between position and momentum and can be interpreted as a Lorentz-invariant natural cutoff [11]. In other words, the concept of minimal physical length appears naturally in QG scenarios by generalization of the ordinary Heisenberg commutator relations between position and momentum in Hilbert space. In this respect, it is important to note that all the above-mentioned approaches to QG can be considered as the origin of GUP, which allow the study of the effects of a minimal length scale in different areas of physics; see Ref. [12] for a detailed review. So, the deformation of Heisenberg's uncertainty principle (HUP), i.e., GUP, is a natural and inevitable consequence of the QG proposal. As an additional motivation for emphasizing the theoretical importance of GUP, let us mention the attempts to resolve the information-loss puzzle in black hole physics by considering GUP; see, for instance, Refs. [11,13–18]. Concerning black hole physics, in Ref. [19] argued that there could be black hole remnants due to GUP. In this direction, the implications of GUP for the complementarity principle proposed for the black hole information-loss paradox are investigated in Ref. [20]. Also, in Ref. [21] it is shown that by taking GUP in the context of extra-dimension theories, there is a possibility of agreeing with the outcomes of LHC, which claims that no black holes are recognizable around 5 TeV [22]. Since a deformation of the Heisenberg uncertainty principle affects various quantum phenomena, some efforts have been made to understand the phenomenological aspects of GUP models in the context of astrophysics, cosmology, and high-energy physics in recent years; see, for instance, Refs. [23–31]. The consequences of GUP for the physics of white dwarf stars are also studied in Refs. [32–34]. Violation of the weak equivalence principle within QM is one of the controversial outcomes of GUP [35,36], confirmed by the deviation reported in neutron interferometry experiments [37].

The lack of a direct experimental test of tentative theories of QG is due to the current limits, both in measurement and in the huge energy required in some experimentally controllable phenomena in the vicinity of the Planck scale. However, this attempt has evolved seriously as one of the major challenges of QG phenomenological studies in recent years; see, for instance, Refs. [38,39]. In the light of proposed experimental tests, the current path of QG could be more coherent since naturally it is expected that some of the proposals involved may be redundant and could even be ruled out. Indeed, it is expected that application of some experimental practicality within the different proposals related to QG will make them more efficient and realizable depending on the engineered improvements in the current designs. Within the last two decades, technical developments in experiments related to phenomenology of quantum gravity and probing spacetime structure at short distances have focused on the control of physical systems at the Planck scale. These attempts were able to provide promising facilities in order to check the correctness of the phenomenological predictions of QG theories [40]. The already-conceived idea of QG tempts one to think that the intersection between QM and GR is too difficult to access through laboratory experiments and seems indeed to be on the other side of the accessible knowledge horizon [41]. In other words, it was assumed that firm predictions are impossible without a fully fledged theory of QG, which combines QM and GR in a new set of laws comparable with observations. However, in a new look at QG phenomenology, which started with the works cited in Refs. [42–45], it is believed that there is the possibility of meeting the theory with experiment even in the absence of a well established, final theory of QG. The new aspect of QG phenomenology can be defensible from the following two perspectives. Firstly, over time, significant progress has been made with empirical techniques that has now made it possible to test the QG effects credibly. Secondly, theoreticians have succeeded in handling some proposals and ideas with permissible prospects that could be tested by common experimental techniques. In a generic sense, the foremost purpose of QG phenomenological studies is to try to suggest some ways of deriving potential experimental signatures from numerous approaches. The modifications arising from QG in the form of relevant GUP affect the Hamiltonians of the systems under study; this is expected to lead to small modifications in measurable quantities in the bed of some physical experiments. So far, numerous attempts have been made to explore spacetime structure at the Planck scale by tuning the characteristic parameter introduced by the relevant QG proposal with experimental data; see Refs. [46–54]. The upper bounds released so far strongly indicate the fact that one needs to look for even more advanced and special experimental setups to detect QG effects with the ideal resolution expected in theory. Of course, the progress made in recent years in coherence between theoretical and experimental aspects of quantum optics, in particular the new approach towards light–matter interactions, has opened a novel direction for testing new areas of physics such as Planck-scale physics with excellent resolution [55–57].

One of the most accurate and trustworthy tools that can be used to explore new areas of physics is *atomic interferometry* (AI), which in its advanced setups exploits *laser-cooled atoms*. It is important to note that, because of the certain sensitivity of AI, it has been used extensively to achieve accurate measurements in physics[1] [61–63]. In recent years we have also been faced with the impressive application of AI for testing fundamental laws and principles of physics [37,64]. Amelino-Camelia et al. were pioneers, proposing the idea that AI [65] can be used for controlling the QG characteristic parameter released in the DSR deformed dispersion relation [66]. This precious idea has motivated us in this paper to investigate the possibility of probing the Planck-scale spacetime with the resolution allowed by a cold rubidium atom embedded in an AI setup, proposed based on a new class of microsystems technology known as *micro-opto-electromechanical systems* (MEOMS)[2], as one of the

[1] AI systems also have some other applications, like that of being developed as accelerometers [58] and gyroscopes [59]. It is interesting to mention that recently such systems were used to map the gravitomagnetic field of the earth in an orbiting satellite [60].

[2] In simple terms, MEOMS is a subset of microsystems technology, which, together with micro-electromechanical systems (MEMS), forms the specialized technology fields using miniaturized combinations of optics, electronics, and mechanics.

most sensitive and accurate measurements performed by AI that plays a central role in our analysis is determination of the *fine structure constant* (FSC) α. In more detail, AI has managed to obtain a value of $\alpha^{-1} = 137.035\,999\,037(91)$ [67], which is the second best value relative to the one concluded from the electron anomaly measurement [68]. This has prompted an investigation of whether AI can provide the possibility of exploring Planck-scale spacetime with improved resolution. In this manuscript, we confront a GUP proposal that contains the most general deformation as proposed in Ref. [69] with cold atom recoil measurement. The proposed study predicts the narrowest constraints, considering all modification terms up to the highest possible order of GUP characteristic scale.

2. Natural cutoff-modified commutation relations: The most general form of modification

Common versions of GUP comprise modification terms containing linear and quadratic momentum operators or combinations thereof [9,10]. Here, we plan to introduce a GUP proposal containing a general deformation function that is expected to address the most general form of modification of the momentum operator. Explicitly, our idea is that, by taking higher powers of momentum in its deformed coordinate representation, phenomenologically there may be the possibility of probing Planck-scale spacetime with an improved resolution.

The most general form of GUP can be suggested through the following commutation relations:

$$[x^i, p_j] = i\hbar\left(\delta^i_j + f[p]^i_j\right), \tag{1}$$

in which $f[p]^i_j$ denotes a tensorial function so that its functional dependence on the momentum strongly depends on the form of the deformed coordinate representation of the momentum operator admitted by various GUP models [69]. By employing an inductive method one can obtain such expressions as

$$p_i \to \tilde{p}_i = p_i\left(1 + \lambda_0 + \lambda_1 (p^j p_j)^{1/2} + \lambda_2 (p^j p_j) + \lambda_3 (p^j p_j)^{3/2} + \lambda_4 (p^j p_j)^2 + \cdots\right), \tag{2}$$

for the most general form of the modified momentum operator. The above expression can also be demonstrated in a more compact form as follows:

$$p_i \to \tilde{p}_i = p_i\left(1 + \sum \lambda_n (p^j p_j)^{n/2}\right), \quad n = 0, 1, 2, 3, \ldots, \tag{3}$$

in which $\lambda_n = \frac{\lambda_0}{(M_p c)^n}$ is the most general form of the GUP characteristic parameter containing the dimensionless constant λ_0. Of course, if we insist on the condition $\lambda_0 > 0$ being satisfied, the most general form of the modified momentum operator (3) is re-expressed as

$$p_i \to \tilde{p}_i = p_i\left(1 \pm \sum \lambda_n (p^j p_j)^{n/2}\right), \quad n = 0, 1, 2, 3, \ldots; \tag{4}$$

in what follows, we focus on this version. Here, it should be stressed that, although in the presentation (3) both cases $\lambda_0 > 0$ and $\lambda < 0$ are possible, due to the form of Eq. (4), we deal only with positive values. From the perspective of phenomenology, it is believed that the GUP parameter should be positive; however, in Refs. [33,70] the possibility of a negative[3] one was also discussed. Theoretically, exploring quantum spacetime cannot be fully achieved unless $\lambda_0 = 1$. This brings the notion that,

[3] According to the literature the possibility of a negative sign for the GUP parameter was first raised in Ref. [71] for formulation on a crystal lattice.

on deriving upper bounds close to unity, the quantum spacetime becomes more accessible, which is a step forward in the direction of testing relevant QG predictions. In Ref. [69], further details can be found on the GUP proposal at hand.

3. Experimental scheme: Inbuilt atom interferometer MEOMS-based optical finesse cavity

The basic principle of this assembly is that the cold ensemble of atoms, when launched inside an optical cavity, splits into two clouds that both traverse different paths based on the laser input. This generates a velocity-based selection of atoms based on their excitation in the hyperfine states, allowing them to recoil backwards or still be defined by the states $|g\rangle$ and $|e\rangle$. The difference between recoiling atoms and steady atoms sets up a number of Bloch oscillations, which transmit the recoiling velocities to the slowed atoms and ensure that the internal state of the atom does not change. The atomic velocity increases by $2u_r$, where u_r is the recoil velocity of the atom when absorbing the momentum of the photon. The final velocity at this stage is the sum of the initial velocity distribution and the N Bloch oscillations. Meanwhile, another Raman pulse is applied to the final velocity, transferring the atoms back to $|g\rangle$. The operation of the proposed system comprises an engineered Fabry–Pérot optical finesse cavity, which is conventionally constituted of two confocal mirrors supporting the free-space propagation of light, while in this design one of the confocal mirrors is replaced by a vibrating micromechanical oscillator. The role of the optical finesse cavity has been broadly discussed in several proposed experiments for probing non-commutative theories and the possible realization of QG phenomena using the current technology. The design of an optical cavity coupled with nano- and micromechanical elements has been reported in previous studies; see Refs. [56,57]. However, in the present study we propose a novel confirmation of the architecture based on the same optical coupling with electromechanical systems, but now introducing an atomic ensemble into the cavity and replacing one of the spherical confocal mirrors with a micromechanical oscillator. We propose the introduction of a micro-electro-opto-mechanical system (MEOMS) component, which, besides electromechanical coupling, provides for the integration of optical components as well for exploring the QG phenomena. This setup is schematically displayed in Fig. 1. The Fabry–Pérot optical cavity amplifies the light on each pass, which creates a laser gain medium in the cavity and limits the frequency noise, adding to its sensitivity to the wavelength of the light. The resonant enhancement in the cavity increases the transitions due to minimum laser power, which otherwise consumes a multi-watt power system. The AI enclosed in the optical cavity limits the wavefront distortions found in conventional systems, which increases its sensitivity and efficiency. One of the pivotal components in the assembly generally described in Fig. 1 is a miniature MEOMS-based oscillator, which also acts as a complementary confocal mirror for the cavity and has been designed in such a way that it acts as a transducing element to pick up the optical signal for the atomic ensemble. The oscillator keeps moving so as to arrest the ensemble during its *Raman transition* between the hyperfine levels. The transition should be coherent with the Bloch oscillation provided by the probe laser, creating about N Bloch oscillations in each run, and the velocity of the atoms could be effectively measured. The periodic motion of the vibrational MEOMS-based oscillator is capable of limiting the spatial variations to reduce the interferometric contrast. The MEOMS-based oscillator is proposed to be made of a freestanding monolayer of molybdenum disulfide (MoS_2), which is known to have an optical bandgap of about 1.6–2 eV and shows strong photoluminescence near the bandgap due to circularly polarized optical pumping. The changes due to atom recoil on the monolayer MoS_2 are detected by the low-power-consumption photodetector and cause minimum scattering and loss [72].

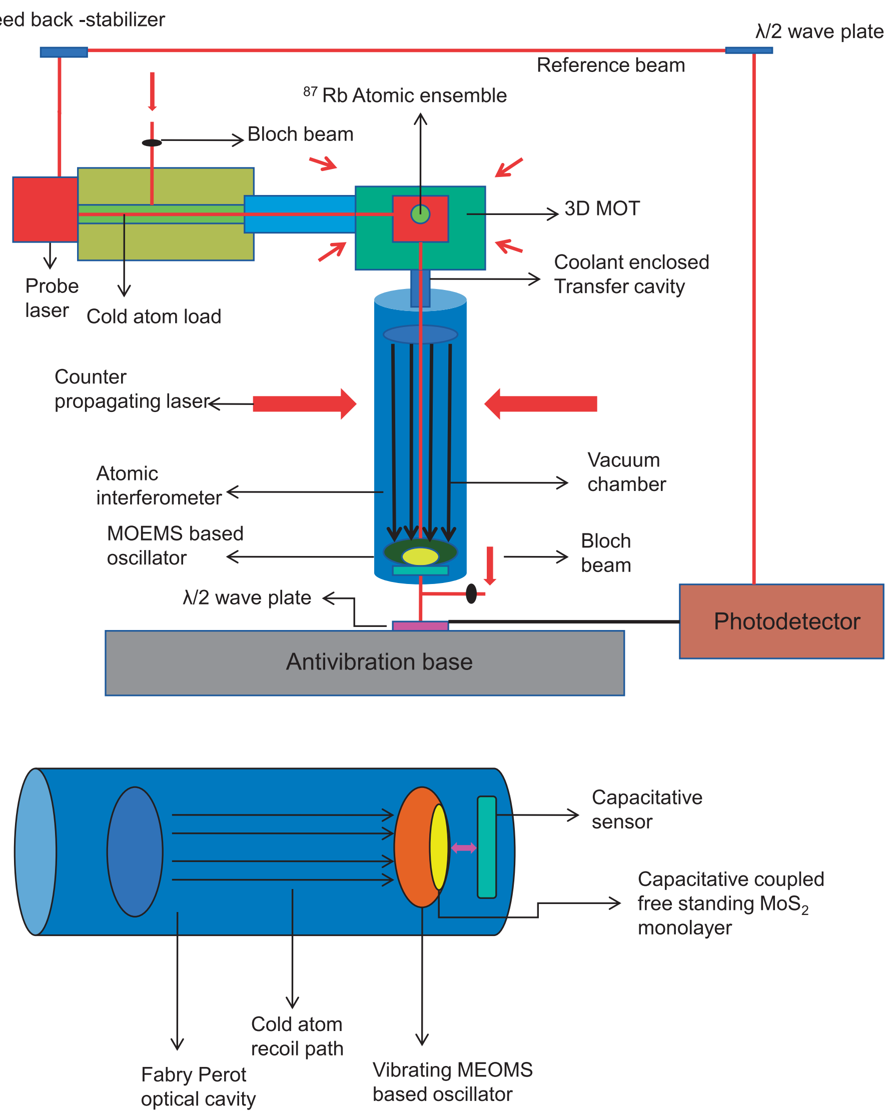

Fig. 1. Schematic representation of an inbuilt atom interferometer MEOMS-based optical finesse cavity.

In this design, the oscillator is attached to the photodetector, which monitors the recoil velocity of the atomic ensemble without affecting the internal state of the atoms. The initial leg of the experiment starts with a 2D-MOT (magneto-optical trap) molasses, which is expected to load the atoms into the system by a slow atomic beam into the hyperfine level $|g\rangle$. Then, using a standard 3D-MOT molasses, it is brought into the vicinity of the optical cavity. The advantage of this architecture is that it allows the combination of a high atomic flux and controlled atomic velocities, which are not precisely provided by conventional use of Zeeman slower or thermal beam devices. As a result, when the cold atoms are pumped into the cavity by the 3D molasses activation, it provides precise control of the velocity in the optical velocity [73]. The velocity adjustments contribute to the flat parabolic atomic trajectories, compensating for the default gravitational acceleration effect. This velocity selection of atoms in the cavity provides for more flexible time-dependent studies like Raman transitions between two hyperfine ground states and a complementary Bloch oscillation; this is schematically displayed in Fig. 2. It is worth mentioning that in this setup the time-dependent noise sources will also be limited, making it potentially more efficient. The atomic source is ^{87}Rb and the ensemble is induced

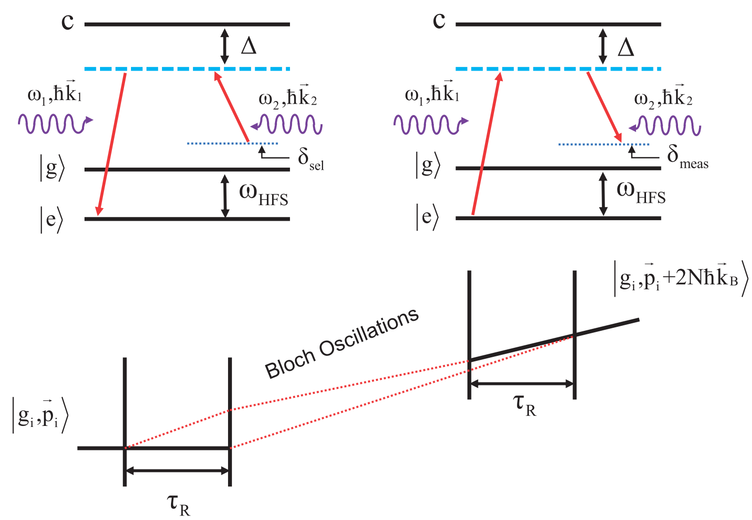

Fig. 2. Schematic representation of Raman transitions between hyperfine levels $|g\rangle$ and $|e\rangle$ along with Bloch oscillations.

into the optical cavity through the MOT arrangements. The atoms exist in between two hyperfine ground states $|g\rangle$ and $|e\rangle$. The atomic ensemble in the optical cavity detects maximum possible recoils due to Raman transitions when two counterpropagating laser beams excite the atoms that are trapped in it after cooling. The Raman frequencies of ω_1 and ω_2 and wave vectors $\vec{k}_1$ and $\vec{k}_2$ create coherent atomic beams in the $|e\rangle$ state where the remaining atoms of the $|g\rangle$ state are tuned to single photon transitions. The reception of these transitions in hyperfine states gives rise to the well defined N Bloch oscillations, which are well received by the MEOM oscillator.

3.1. *Formulation*

Now we formulate the above description mathematically. The energy conservation law imposes the following equality at resonance:

$$\hbar(\omega_1 - \omega_2 - \omega_{\rm HFS}) = \hbar\Delta + \frac{[\hbar(\vec{k}_1 - \vec{k}_2) + m\vec{u}_i]^2 - m^2\vec{u}_i^2}{2m}\,. \tag{5}$$

Here, the quantities m, Δ, and $\hbar\omega_{\rm HFS} = E_{g_1} - E_{g_2}$ refer to the mass of atoms, the single photon setting of the atomic levels, and the energy difference between the hyperfine levels $|g\rangle$, $|e\rangle$, respectively. By defining $\delta_{\rm sel} \equiv \omega_1 - \omega_2 - \omega_{\rm HFS}$ as a Raman transition setting, the above conservation equation takes the following form:

$$\delta_{\rm sel} = \Delta + \frac{\hbar}{2m}(\vec{k}_1 - \vec{k}_2)^2 + (\vec{k}_1 - \vec{k}_2)\cdot\vec{u}_i\,. \tag{6}$$

In order to transfer the high recoil velocities to atoms in a short time, so that the relevant hyperfine internal state of atoms does not change after the process of velocity selection, the number of N Bloch oscillations comes into play. Every Bloch oscillation separately increases the atomic velocity by a factor of $2\vec{u}_r$, where $\vec{u}_r = \frac{\hbar\vec{k}_{\rm B}}{m}$ refers to the recoil velocity of the atom while absorbing a photon with the relevant momentum $\hbar\vec{k}_{\rm B}$. As a result, the final velocity attributed to the atoms can be denoted by $\vec{u}_f = \vec{u}_i + 2N\vec{u}_r$. In the second pair of Raman $\frac{\pi}{2}$ pulses, the final velocity distribution is centered on $\vec{u}_f$. In addition, by applying the energy conservation law, the Raman regulation for the velocity measurement here reads as

$$\delta_{\rm meas} = \Delta + \frac{\hbar}{2m}(\vec{k}_1 - \vec{k}_2)^2 + (\vec{k}_1 - \vec{k}_2)\cdot\vec{u}_f \,, \tag{7}$$

where, by subtracting it from Eq. (6), one gets

$$|\delta_{\rm sel} - \delta_{\rm meas}| = (k_1 + k_2)|u_f - u_i|. \tag{8}$$

Now the ratio of the Planck constant to the mass of the atoms, i.e., $\frac{h}{m}$, is found by

$$\frac{h}{m} = \frac{2\pi\,|\delta_{\rm sel} - \delta_{\rm meas}|}{2Nk_{\rm B}(k_1 + k_2)}, \tag{9}$$

which addresses the FSC α via the following well known relation:

$$\alpha^2 = \frac{2R_\infty}{c}\frac{m}{m_e}\frac{h}{m} \,. \tag{10}$$

Here, R_∞, m_e, and c are the Rydberg constant, the electron mass, and the speed of light, respectively. In Ref. [67], by the consideration of ^{87}Rb atoms, the authors performed an excellent measurement of $\frac{\hbar}{m}$, which, after an approximate margin of error, has given a value of $\frac{h}{m_{\rm Rb}} = 4.591\,359\,2729(57)\times 10^{-9}\,{\rm m^2\,s^{-1}}$. In this measurement the role of the internal hyperfine levels $|g\rangle$ and $|e\rangle$ lies in the $5{\rm S}_{\frac{1}{2}}$ $|F=2, m_F=0\rangle$ and $5{\rm S}_{\frac{1}{2}}$ $|F=1, m_F=0\rangle$ states of ^{87}Rb atoms, respectively. As a necessary piece of information in this measurement, an atomic beam with an initial velocity $u_i = 20\,{\rm m\,s^{-1}}$, was prepared in the $F=2$ hyperfine level. A Ti sapphire laser with relevant wavelength $\lambda_B = \frac{2\pi}{k_{\rm B}} = 532$ nm was produced, which could produce $N = 500$ Bloch oscillations for the application on ^{87}Rb atoms in each run.

4. Explicit constraints for the Planck-scale characteristic parameter

4.1. The case without superposition of the GUP-modified terms

Here we address the GUP modifications in terms of different values of n separately. For clarity, we assume that there is no superposition of the GUP modification term, which perceives each GUP modification term to be considered separately in the absence of other possible terms.

By setting $n = 0$, Eq. (4) reads as

$$p_i \to \tilde{p}_i = p_i(1 \pm \lambda_0) \,. \tag{11}$$

In this new representation, the Hamiltonian related to a 1D quantum system can be expanded as

$$H_{{\rm GUP}(n=0)} = (1 + \lambda_0^2 \pm 2\lambda_0)\frac{p^2}{2m} + V(x) \,. \tag{12}$$

By applying the above GUP-modified Hamiltonian to the cold ^{87}Rb atoms, the relevant GUP term modifies the kinetic energy of the ^{87}Rb atoms as follows:

$$E_{K-{\rm GUP}(n=0)} = (1 + \lambda_0^2 \pm 2\lambda_0)\frac{p^2}{2m_{\rm Rb}}. \tag{13}$$

According to the prior pattern, here the GUP counterpart of Eq. (8) takes the following form:

$$|\delta_{\rm sel} - \delta_{\rm meas}|_{{\rm GUP}(n=0)} = (1 \pm \lambda_0)^2(k_1 + k_2)|u_f - u_i| \,; \tag{14}$$

by putting this into Eqs. (9) and (10), we finally arrive at

$$\alpha^{-1}_{\mathrm{GUP}(n=0)} = \left(\frac{2R_\infty}{c}.\frac{m_u}{m_e}.\frac{h}{m_{\mathrm{Rb}}}(1 \pm \lambda_0)^2\right)^{-\frac{1}{2}}. \tag{15}$$

Given that the setup at hand is a low-energy quantum system, by estimating the GUP effect on the FSC via the following relation, one can derive an explicit upper bound for λ_0:

$$\frac{|\alpha^{-1}_{\mathrm{GUP}} - \alpha^{-1}|}{\alpha^{-1}} < \text{measurement accuracy of } \alpha^{-1}. \tag{16}$$

This relation expresses the fact that by taking into the account the measurement of α^{-1} with a precision order of magnitude of 2.5×10^{-10} [68], one can constrain the value of λ_0, so that it will still be valid for the measurement of α^{-1} in the presence of QG effects. This is known as a bottom-up QG phenomenological approach, on which our analysis in this study is based. Indeed, an interesting idea transposed into this approach is that, relying on data due to low-energy phenomena, there is the possibility of probing Planck-scale spacetime with different resolutions depending on the relevant precision measurements. Now by setting values of $R_\infty = 10\,973\,731.565\,839(55)\,\mathrm{m}^{-1}$, $m_{\mathrm{Rb}} = 86.909\,180\,535(10)m_u$, $m_e = 5.485\,799\,0946(22) \times 10^{-4}m_u$, $M_p \sim 1.3 \times 10^{19}m_u$, $c = 3 \times 10^8\,\mathrm{m\,s}^{-1}$, the following results are obtained for bounds on λ_0:

$$-2 < \lambda_0 < -1 \tag{17}$$

and

$$1 < \lambda_0 < 2, \tag{18}$$

for two cases of positive and negative signs, respectively. As we have mentioned previously, the condition $\lambda_0 > 0$ should be satisfied. So, the first constraint is rejected.

By setting $n = 1$, Eq. (4) in one dimension reads as

$$p \to \tilde{p} = p(1 \pm \lambda_1 p), \quad \lambda_2 = \frac{\lambda_0}{(M_p c)}. \tag{19}$$

In this new representation, by keeping all powers of λ_0, the relevant GUP-modified kinetic energy of ^{87}Rb atoms can also be written as

$$E_{K-\mathrm{GUP}(n=1)} = \frac{p^2}{2m_{\mathrm{Rb}}} + \lambda_0^2\frac{p^4}{2m_{\mathrm{Rb}}(M_p c)^2} \pm \lambda_0\frac{p^3}{m_{\mathrm{Rb}}(M_p c)}. \tag{20}$$

Here the GUP counterpart of Eq. (8) takes the following form:

$$|\delta_{\mathrm{sel}} - \delta_{\mathrm{meas}}|_{\mathrm{GUP}(n=1)} = (k_1+k_2)|u_f - u_i| + \frac{2m^2_{\mathrm{Rb}}\lambda_0^2(k_1+k_2)}{(M_p c)^2}(u_f^3 - u_i^3) \pm \frac{3m_{\mathrm{Rb}}\lambda_0(k_1+k_2)}{(M_p c)}(u_f^2 - u_i^2); \tag{21}$$

by putting this into Eqs. (9) and (10), we finally arrive at

$$\alpha^{-1}_{\mathrm{GUP}(n=1)} = \left[\frac{2R_\infty}{c}\frac{m_u}{m_e}\frac{h}{m_{\mathrm{Rb}}}\left(1 + \frac{2(\frac{m_{\mathrm{Rb}}}{m_u})^2\lambda_0^2}{(\frac{M_p}{M_u}c)^2}(u_f^2 + u_i u_f + u_i^2) \pm \frac{3\frac{m_{\mathrm{Rb}}}{m_u}\lambda_0}{(\frac{M_p}{M_u}c)}(u_f + u_i)\right)\right]^{-\frac{1}{2}}. \tag{22}$$

Using the method described above, we obtain the following upper bounds on λ_0:

$$1 \leq \lambda_0 < 1.5 \times 10^{14} \tag{23}$$

and

$$1 \leq \lambda_0 < 4 \times 10^{23} \tag{24}$$

for two cases of positive and negative signs, respectively.

By setting $n = 2$, Eq. (4) in one dimension reads as

$$p \to \tilde{p} = p(1 \pm \lambda_2 p^2), \quad \lambda_2 = \frac{\lambda_0}{(M_p c)^2} \, . \tag{25}$$

Here also, by keeping all powers of λ_0, the relevant GUP-modified kinetic energy of ^{87}Rb atoms is presented as follows:

$$E_{K-\mathrm{GUP}(n=2)} = \frac{p^2}{2m_{\mathrm{Rb}}} + \lambda_0^2 \frac{p^6}{2m_{\mathrm{Rb}}(M_p c)^4} \pm \lambda_0 \frac{p^4}{m_{\mathrm{Rb}}(M_p c)^2}, \tag{26}$$

which results in the following modified expression for Eq. (8):

$$|\delta_{\mathrm{sel}} - \delta_{\mathrm{meas}}|_{\mathrm{GUP}(n=2)} = (k_1 + k_2)|u_f - u_i| + \frac{3m_{\mathrm{Rb}}^4 \lambda_0^2 (k_1 + k_2)}{(M_p c)^4}(u_f^5 - u_i^5) \pm \frac{4m_{\mathrm{Rb}}\lambda_0(k_1 + k_2)}{(M_p c)^2}(u_f^3 - u_i^3) \, . \tag{27}$$

Putting this into Eqs. (9) and (10), we arrive at

$$\alpha^{-1}_{\mathrm{GUP}(n=2)} = \left[\frac{2R_\infty}{c}\frac{m_u}{m_e}\frac{h}{m_{\mathrm{Rb}}}\left(1 + \frac{3(\frac{m_{\mathrm{Rb}}}{m_u})^4\lambda_0^2}{(\frac{M_p}{M_u}c)^4}\frac{u_f^5 - u_i^5}{u_f - u_i} \pm \frac{4(\frac{m_{\mathrm{Rb}}}{m_u})^2\lambda_0}{(\frac{M_p}{M_u}c)^2}(u_f^2 + u_i u_f + u_i^2)\right)\right]^{-\frac{1}{2}} . \tag{28}$$

Using the method described previously, we obtain the following upper bounds on λ_0:

$$1 \leq \lambda_0 < 1.4 \times 10^{38}, \tag{29}$$

and

$$1 \leq \lambda_0 < 3.2 \times 10^{47}, \tag{30}$$

for two cases of positive and negative signs, respectively.

By setting $n = 3$, Eq. (4) in one dimension reads as

$$p \to \tilde{p} = p(1 \pm \lambda_3 p^3), \quad \lambda_3 = \frac{\lambda_0}{(M_p c)^3} \, . \tag{31}$$

In the same way, for the relevant GUP-modified kinetic energy of ^{87}Rb atoms, we have

$$E_{K-\mathrm{GUP}(n=3)} = \frac{p^2}{m_{\mathrm{Rb}}} + \lambda_0^2 \frac{p^8}{2m_{\mathrm{Rb}}(M_p c)^6} \pm \lambda_0 \frac{p^5}{m_{\mathrm{Rb}}(M_p c)^3} \, . \tag{32}$$

In the presence of the relevant GUP modification, Eq. (8) is rewritten as

$$|\delta_{\mathrm{sel}} - \delta_{\mathrm{meas}}|_{\mathrm{GUP}(n=3)} = (k_1 + k_2)|u_f - u_i| + \frac{8m_{\mathrm{Rb}}^6 \lambda_0^2 (k_1 + k_2)}{2(M_p c)^6}(u_f^7 - u_i^7) \pm \frac{5m_{\mathrm{Rb}}\lambda_0(k_1 + k_2)}{(M_p c)^3}(u_f^5 - u_i^5) \, ; \tag{33}$$

by putting this into Eqs. (9) and (10), we come to

$$\alpha^{-1}_{\mathrm{GUP}(n=3)} = \left[\frac{2R_\infty}{c}\frac{m_u}{m_e}\frac{h}{m_{\mathrm{Rb}}}\left(1+\frac{4(\frac{m_{\mathrm{Rb}}}{m_u})^6\lambda_0^2}{(\frac{M_p}{M_u}c)^6}\frac{u_f^7-u_i^7}{u_f-u_i}\pm\frac{5(\frac{m_{\mathrm{Rb}}}{m_u})^3\lambda_0}{(\frac{M_p}{M_u}c)^3}(u_f^3+u_i^2u_f+u_iu_f^2+u_i^3)\right)\right]^{-\frac{1}{2}}. \tag{34}$$

Once again, via the method described above, we obtain other upper bounds on λ_0 as follows:

$$1 \leq \lambda_0 < 1.5\times 10^{62}, \tag{35}$$

and

$$1 \leq \lambda_0 < 3.3\times 10^{71}, \tag{36}$$

for two cases of positive and negative signs, respectively.

Comparing these obtained constraints for different values of n clearly shows that by considering higher-order powers of momentum in the deformed coordinate representation and neglecting all lower-order terms in the momentum in each step, the possibility for accurate resolution of the spacetime structure on the Planck scale reduces for higher-order terms.

4.2. *The case with superposition of the GUP-modified terms*

Here, unlike the previous subsection, we treat a general form of GUP as a superposition of all possible modification terms (we restrict ourselves to $n = 0, 1, 2, 3$). In this regard, for the 1D system Eq. (4) takes the following form:

$$p \to \tilde{p} = p\left(1 \pm \lambda_0 \pm \lambda_1 p \pm \lambda_2 p^2 \pm \lambda_3 p^3 \pm \cdots\right). \tag{37}$$

In this case, the quantities E_K, $|\delta_{\mathrm{sel}} - \delta_{\mathrm{meas}}|$, and α^{-1} can be modified in the following forms:

$$\begin{aligned} E_{K-\mathrm{GUP}(\pm)} = \frac{1}{2m_{\mathrm{Rb}}}\Big[&(1\pm\lambda_0)^2p^2 + (2\lambda_0\lambda_1 \pm 2\lambda_1)p^3 + (\lambda_1^2 + 2\lambda_0\lambda_2 \pm 2\lambda_2)p^4 \\ &+ (2\lambda_0\lambda_3 + 2\lambda_1\lambda_2 \pm 2\lambda_3)p^5 + (\lambda_2^2 + 2\lambda_1\lambda_3)p^6 + 2\lambda_2\lambda_3 p^7 + \lambda_3^2 p^8\Big], \end{aligned} \tag{38}$$

$$\begin{aligned} |\delta_{\mathrm{sel}} - \delta_{\mathrm{meas}}|_{\mathrm{GUP}(\pm)} = &(1\pm\lambda_0)^2(k_1+k_2)|u_f-u_i| + 6m_{\mathrm{Rb}}(\lambda_0\lambda_1 \pm \lambda_1)(k_1+k_2)(u_f^2-u_i^2) \\ &+ 2m_{\mathrm{Rb}}^2(\lambda_1^2 + 2\lambda_0\lambda_2 \pm 2\lambda_2)(k_1+k_2)(u_f^3-u_i^3) \\ &+ 5m_{\mathrm{Rb}}^3(\lambda_0\lambda_3 + \lambda_1\lambda_2 \pm \lambda_3)(k_1+k_2)(u_f^4-u_i^4) \\ &+ 9m_{\mathrm{Rb}}^4(2\lambda_1\lambda_3 + \lambda_2^2)(k_1+k_2)(u_f^5-u_i^5) \\ &+ 14m_{\mathrm{Rb}}^5\lambda_2\lambda_3(k_1+k_2)(u_f^6-u_i^6)4m_{\mathrm{Rb}}^6\lambda_2\lambda_3(k_1+k_2)(u_f^7-u_i^7), \end{aligned} \tag{39}$$

and

$$\alpha^{-1}_{\mathrm{GUP}(\pm)} = \Bigg[\frac{2R_\infty}{c}\frac{m_u}{m_e}\frac{h}{m_{\mathrm{Rb}}}\Bigg(1+(1\pm\lambda_0)^2+6\frac{m_{\mathrm{Rb}}}{m_u}(\lambda_0\lambda_1\pm\lambda_1)(u_f+u_i)$$
$$+2\left(\frac{m_{\mathrm{Rb}}}{m_u}\right)^2(\lambda_1^2+2\lambda_0\lambda_2\pm 2\lambda_2)(u_f^2+u_iu_f+u_i^2)$$
$$+5\left(\frac{m_{\mathrm{Rb}}}{m_u}\right)^3(\lambda_0\lambda_3+\lambda_1\lambda_2\pm\lambda_3)(\frac{u_f^4-u_i^4}{u_f-u_i})+9\left(\frac{m_{\mathrm{Rb}}}{m_u}\right)^4(\lambda_2^2+2\lambda_1\lambda_3)\left(\frac{u_f^5-u_i^5}{u_f-u_i}\right)$$
$$+14\left(\frac{m_{\mathrm{Rb}}}{m_u}\right)^5\lambda_2\lambda_3\left(\frac{u_f^6-u_i^6}{u_f-u_i}\right)+4\left(\frac{m_{\mathrm{Rb}}}{m_u}\right)^6\lambda_2\lambda_3\left(\frac{u_f^7-u_i^7}{u_f-u_i}\right)\Bigg)\Bigg]^{-\frac{1}{2}}, \quad (40)$$

respectively. By setting $\lambda_2 = \lambda_1^2$ and $\lambda_3 = \lambda_1^3$, the following upper bounds on λ_0 are achieved:

$$-1.000\,02 < \lambda_0 < -0.999\,978 \quad (41)$$

and

$$0.999\,978 < \lambda_0 < 1.000\,02 \quad (42)$$

for the cases of positive and negative signs, respectively. The case with negative λ_0 is not acceptable, as we have discussed previously. The condition (42) is very tightly bound on the quantum gravity parameter, λ_0. So, in this proposed setup one is able to probe the quantum spacetime structure even in the low-energy regime. This is so important in testing the QG proposal in the laboratory on the energy scales accessible today.

5. Summary

To summarize, in this work, via accessible low-energy technology, we have found a possibility of probing the quantum spacetime structure with a favorable theoretical resolution. Concerning the GUP proposal containing the most general modification of coordinate representation of the momentum operator, we have studied how to use the outcomes from ^{87}Rb CARE (especially the measurement of FSC) schematically designed in Figs. 1 and 2 to constrain the relevant dimensionless QG characteristic parameter λ_0. By enclosing the underlying AI setup within a high-finesse optical cavity, which is supported by a new class of low-power-consumption integrated devices known as MEOMS, it has been distinguished from conventional architectures. MEOMS belong to the family of microsystems technology that, along with electromechanical energy, harness the low-dimension optics. As a distinct factor in this setup, the presence of a micro-mechanical oscillator instead of spherical confocal mirrors as one of the components of the high-finesse optical cavity should be pointed out.

Altogether, this study has been done in two ways: with and without superposition of separate modification terms in momentum. The first step was based on the assumption that there is no superposition of modification terms so that each term is considered individually in the absence of other possible terms. In this way, the best constraint on λ_0 is extracted as $1 \leq \lambda_0 < 2$, which, in the deformed coordinate representation, makes the momentum operator appear as a rescaled quantity. However, the constraints explicitly reflect the fact that by increasing the power of momentum in the deformed coordinate representation the resolution for exploring the spacetime structure in Planck's scale reduces and becomes much weaker.

In contrast to the first step, in the next step we considered a general form of GUP as a superposition of all possible modification terms (we preferred to consider just the first four terms with $n = 0, 1, 2, 3$). We have obtained a strict and tight constraint as $0.999\,978 < \lambda_0 < 1.000\,02$, which is very favorable from the theoretical perspective. This constraint obviously challenges the long-lived belief in QG phenomenology projects that probing the quantum spacetime structure is possible just by having full access to the Planck energy. In other words, this setup paves a novel way for probing Planck-scale spacetime procured by accessible low-energy technology, in particular the proposed opto-atomic ^{87}Rb interferometric arrangement. So, one may argue that the best playground to test QG is not just high-energy physics; a table-top nanosystem assembly can act as well.

Acknowledgements

The work of K.N. is financially supported by the Research Institute for Astronomy and Astrophysics of Maragha (RIAAM) under research project No. 1/5440-67.

Funding

Open Access funding: SCOAP^3.

References

[1] S. Hossenfeldera, M. Bleicher, S. Hofmann, J. Ruppert, S. Scherer, and H. Stöcker, Phys. Lett. B **575**, 85 (2003).
[2] R. Hedrich, arXiv:0902.0190 [gr-qc] [Search INSPIRE].
[3] D. J. Gross and P. F. Mendle, Nucl. Phys. B **303**, 407 (1988).
[4] K. Konishi, G. Paffuti, and P. Provero, Phys. Lett. B **234**, 276 (1990).
[5] C. Rovelli and L. Smolin, Nucl. Phys. B **442**, 593 (1995).
[6] A. Ashtekar and J. Lewandowski, Class. Quantum Grav. **14**, A55 (1997).
[7] G. Amelino-Camelia, Int. J. Mod. Phys. D **11**, 1643 (2002).
[8] J. Magueijo and L. Smolin, Phys. Rev. Lett. **88**, 190403 (2002).
[9] A. F. Ali, S. Das, and E. C. Vagenas, Phys. Lett. B **678**, 497 (2009).
[10] S. Das, E. C. Vagenas, and A. F. Ali, Phys. Lett. B **690**, 407 (2010).
[11] A. Kempf, G. Mangano, and R. B. Mann, Phys. Rev. D **52**, 1108 (1995).
[12] S. Hossenfelder, Living Rev. Relat. **16**, 2 (2013).
[13] A. Kempf and G. Mangano, Phys. Rev. D **55**, 7909 (1997).
[14] A. Kempf, J. Phys. A: Math. Gen. **30**, 2093 (1997).
[15] D. Amati, M. Ciafaloni, and G. Veneziano, Phys. Lett. B **216**, 41 (1989).
[16] M. Maggiore, Phys. Lett. B **304**, 65 (1993).
[17] M. Maggiore, Phys. Lett. B **319**, 83 (1993).
[18] M. Maggiore, Phys. Rev. D **49**, 5182 (1994).
[19] R. J. Adler, P. Chen, and D. I. Santiago, Gen. Relat. Gravit. **33**, 2101 (2001).
[20] P. Chen, Y. C. Ong, and D.-h. Yeom, J. High Energy Phys. **1412**, 021 (2014).
[21] A. F. Ali, J. High Energy Phys. **1209**, 067 (2012).
[22] V. Khachatryan et al. [CMS Collaboration], Phys. Lett. B **697**, 434 (2011).
[23] Y. Sabri and K. Nouicer, Class. Quantum Grav. **29**, 215015 (2012).
[24] M. Khodadi, K. Nozari, and A. Hajizadeh, Phys. Lett. B **770**, 556 (2017).
[25] N. Khosravi and H. R. Sepangi, J. Cosmol. Astropart. Phys. **0804**, 011 (2008).
[26] N. Khosravi and H. R. Sepangi, Phys. Lett. A **372**, 3356 (2008).
[27] A. Tawfik, H. Magdy, and A. F. Ali, Gen. Relat. Gravit. **45**, 1227 (2013).
[28] M. A. Gorji, Phys. Lett. B **760**, 769 (2016).
[29] M. Khodadi, K. Nozari, and H. R. Sepangi, Gen. Relat. Gravit. **48**, 166 (2016).
[30] M. Khodadi and K. Nozari, Ann. Phys. **528**, 785 (2016).

[31] M. Khodadi, K. Nozari, and E. N. Saridakis, Class. Quantum Grav. **35**, 015010 (2018).
[32] R. Rashidi, Ann. Phys. **374**, 434 (2016).
[33] Y. C. Ong, J. Cosmol. Astropart. Phys. **1809**, 015 (2018).
[34] D. K. Mishra and N. Chandra, arXiv:1803.06640 [gr-qc] [Search INSPIRE].
[35] V. M. Tkachuk, Phys. Rev. A **86**, 062112 (2012).
[36] S. Ghosh, Class. Quantum Grav. **31**, 025025 (2014).
[37] L. Zhou et al., Phys. Rev. Lett. **115**, 013004 (2015).
[38] G. Amelino-Camelia, Living Rev. Relat. **16**, 5 (2013).
[39] S. Hossenfelder, arXiv:1010.3420 [gr-qc] [Search INSPIRE].
[40] J. Stachel, *Early History of Quantum Gravity, Black Holes, Gravitational Radiation and the Universe*, eds. B. Iyer and B. Bhawal (Kluwer, Dordrecht, 1999).
[41] G. Amelino-Camelia, Lect. Notes Phys. **541**, 1 (2000).
[42] G. Amelino-Camelia, J. Ellis, N. E. Mavromatos, D. V. Nanopoulos, and S. Sarkar, Nature **393**, 763 (1998).
[43] D. V. Ahluwalia, Mod. Phys. Lett. A **13**, 1393 (1998).
[44] G. Amelino-Camelia, Nature **398**, 216 (1999).
[45] G. F. Giudice, R. Rattazzi, and J. D. Wells, Nucl. Phys. B **544**, 3 (1999).
[46] S. Das and E. C. Vagenas, Phys. Rev. Lett. **101**, 221301 (2008).
[47] P. Pedram, K. Nozari, and S. H. Taheri, J. High Energy Phys. **1103**, 093 (2011).
[48] A. F. Ali, S. Das, and E. C. Vagenas, Phys. Rev. D **84**, 044013 (2011).
[49] P. Wang, H. Yang, and X. Zhang, Phys. Lett. B **718**, 265 (2012).
[50] E. Castellanos and G. Chacón-Acosta, Phys. Lett. B **722**, 119 (2013).
[51] S. Ghosh, Class. Quantum Grav. **31**, 025025 (2014).
[52] S. Jalalzadeh, M. A. Gorji, and K. Nozari, Gen. Relat. Gravit. **46**, 1632 (2014).
[53] K. Nozari, M. Khodadi, and M. A. Gorji, Europhys. Lett. **112**, 60003 (2015).
[54] G. Chacón-Acosta and H. H. Hernandez-Hernandez, Int. J. Mod. Phys. D **24**, 1550033 (2015).
[55] I. Pikovski, M. R. Vanner, M. Aspelmeyer, M. S. Kim, and Č. Brukner, Nat. Phys. **8**, 393 (2012).
[56] S. Dey, A. Bhat, D. Momeni, M. Faizal, A. F. Ali, T. K. Dey, and A. Rehman, Nucl. Phys. B **924**, 578 (2017).
[57] M. Khodadi, K. Nozari, S. Dey, A. Bhat and M. Faizal, Sci. Rep. **8**, 1659 (2018).
[58] A. Peters, K. Y. Chung, and S. Chu, Nature **400**, 849 (1999).
[59] T. L. Gustavson, A. Landragin, and M. A. Kasevich, Class. Quantum Grav. **17**, 2385 (2000).
[60] C. Jentsch, T. Müller, E. M. Rasel, and W. Ertmer, Gen. Relat. Gravit. **36**, 2197 (2004).
[61] P. Cladé, E. de Mirandes, M. Cadoret, S. Guellati-Khélifa, C. Schwob, F. Nez, L. Julien, and F. Biraben, Phys. Rev. A **74**, 052109 (2006).
[62] D. Gao and M. Zhan, Phys. Rev. A **94**, 013607 (2016).
[63] A. D. Cronin, J. Schmiedmayer, and D. E. Pritchard, Rev. Mod. Phys. **81**, 1051 (2009).
[64] R. Geiger and M. Trupke, Phys. Rev. Lett. **120**, 043602 (2018).
[65] A. Wicht et al., Phys. Scr. **102**, 82 (2002).
[66] G. Amelino-Camelia, C. Lämmerzahl, F. Mercati, and G. M. Tino, Phys. Rev. Lett. **103**, 171302 (2009); **104**, 039901 (2010) [erratum].
[67] R. Bouchendira, P. Cladé, S. Guellati-Khélifa, F. Nez, and F. Biraben, Phys. Rev. Lett. **106**, 080801 (2011).
[68] T. Aoyama, M. Hayakawa, T. Kinoshita, and M. Nio, Phys. Rev. Lett. **109**, 111807 (2012).
[69] S. Masood, M. Faizal, Z. Zaz, A. F. Ali, J. Raza, and M. B. Shah, Phys. Lett. B **763**, 218 (2016).
[70] Y. C. Ong and Y. Yao, Phys. Rev. D **98**, 126018 (2018).
[71] P. Jizba, H. Kleinert, and F. Scardigli, Phys. Rev. D **81**, 084030 (2010).
[72] G. Kioseoglou, A. T. Hanbicki, M. Currie, A. L. Friedman, D. Gunlycke, and B. T. Jonker, Appl. Phys. Lett. **101**, 221907 (2012).
[73] T. Müller, M. Gilowski, M. Zaiser, P. Berg, Ch. Schubert, T. Wendrich, W. Ertmer, and E. M. Rasel, Eur. Phys. J. D **53**, 273 (2009).